

Theory of antiferromagnetic short-range order in the two-dimensional Heisenberg model

S. Winterfeldt* and D. Ihle

Institut für Theoretische Physik, Universität Leipzig, D-04109 Leipzig, Germany

(Received 24 February 1997)

We present a spin-rotation-invariant theory of short-range order in the square-lattice $S=1/2$ Heisenberg antiferromagnet based on the Green's-function projection technique for the dynamic spin susceptibility. By a generalized mean-field approximation and taking appropriate conditions for two vertex parameters, the static spin susceptibility, the antiferromagnetic correlation length, and the two-spin correlation functions of arbitrary range are calculated self-consistently over the whole temperature region. A good agreement with Monte Carlo results is found. The theory generalizes previous isotropic spin-wave approaches and provides an improved interpolation between the low-temperature and high-temperature behavior of the uniform static susceptibility. Comparing the theory with neutron-scattering data for the correlation length and magnetic susceptibility experiments on La_2CuO_4 , a good quantitative agreement in the temperature dependences is obtained. The fit of the exchange energy yields $J=133$ meV. [S0163-1829(97)05433-7]

I. INTRODUCTION

In high- T_c copper oxides there exist strong antiferromagnetic (AFM) spin correlations¹ probed, for example, by neutron-scattering experiments^{2,3} and by the normal-state magnetic susceptibility $\chi(T,x)$ of $\text{La}_{2-x}\text{Sr}_x\text{CuO}_4$.⁴ The maximum in the temperature dependence of χ (for $x<0.2$) as well as in the doping dependence may be ascribed to AFM short-range order (SRO) which decreases with increasing temperature and doping. Those experiments are calling for a microscopic theory of SRO to describe the dynamic spin susceptibility $\chi(\mathbf{q},\omega;T,x)$ over the whole range of variables on the basis of two-dimensional (2D) correlation models. Frequently, the t - J model is used, where the undoped compounds (e.g., La_2CuO_4) are well described by the $S=1/2$ AFM Heisenberg model on the square lattice,

$$H = \frac{J}{2} \sum_{\langle i,j \rangle} \mathbf{S}_i \mathbf{S}_j. \quad (1)$$

As indicated by many theories and numerical studies,⁵ the ground state of the 2D Heisenberg antiferromagnet has AFM long-range order which (according to the Mermin-Wagner theorem) disappears at nonzero temperatures. At $T>0$ the system is in a paramagnetic phase with AFM SRO. A theory for the cuprates that starts from the Heisenberg limit (1) of the t - J model is desired to describe SRO at all temperatures.

However, most of the existing analytical approaches to the Heisenberg model are valid only at sufficiently low temperatures. For example, Chakravarty *et al.*⁶ have mapped the long-wavelength and low-temperature behavior of Eq. (1) onto the 2D quantum nonlinear σ model in the renormalized classical region (realized in the case of Néel order at $T=0$). Their result for the AFM correlation length for $T \ll 2\pi\rho_s$ (ρ_s is the spin stiffness) obtained by a two-loop renormalization-group analysis⁶ was improved by Hasenfratz and Niedermayer.⁷ Furthermore, the modified spin-wave theories by Takahashi⁸ and Hirsch *et al.*⁹ as well as the Schwinger-boson mean-field theory by Arovas and Auerbach¹⁰ hold only for $T/J \lesssim 0.7$.

The isotropic spin-wave theories by Shimahara and Takada¹¹ (based on an equation-of-motion decoupling) and by Sokol *et al.*¹² (employing a linearization procedure) interpolate between low and high temperatures. It is, however, difficult to extend those approaches by going beyond the mean-field approximation or by including the transfer term in the t - J model. For example, the Green's-function decoupling by Shimahara and Takada^{11,13} only holds in the parameter region $t \ll J$, being unrealistic for the cuprates.

In developing a spin-rotation-invariant theory of SRO which is applicable over the whole temperature region, the projection technique for Green's functions^{14,15} has the advantage to provide a more systematic description of spin correlations and to allow straightforward extensions (e.g., to describe damping effects) as compared with the approaches of Refs. 11–13.

In this paper we present a theory of SRO for the 2D Heisenberg antiferromagnet based on a Green's-function projection method to calculate the dynamic spin susceptibility $\chi(\mathbf{q},\omega;T)$ and spin-correlation functions of arbitrary range. The generalized mean-field approximation within our approach yields an improved interpolation between the low-temperature and high-temperature limits in comparison with Refs. 11 and 12. Our main goals are to compare the theory with available Monte Carlo (MC) data and with experiments on La_2CuO_4 .

The paper is organized as follows. In Sec. II, the Green's-function projection method is applied to the calculation of the dynamic spin susceptibility in a generalized mean-field approximation. In Sec. III, the ground state is investigated, and appropriate conditions for the temperature-dependent vertex parameters in our mean-field decoupling are given. At $T=0$, the two-spin correlation functions and the spin-wave spectrum are compared with projector MC data. In Sec. IV, we present our finite-temperature results on the static susceptibility, the AFM correlation length, the spin structure factor, and the spin-correlation functions of arbitrary range. The results are compared with MC data and with experiments on La_2CuO_4 (correlation length, magnetic susceptibility). The summary of our work can be found in Sec. V.

II. GREEN'S-FUNCTION PROJECTION METHOD

Let us first outline the general scheme of the projection technique for Green's functions based on the equation-of-motion method along the lines indicated by Tserkovnikov.¹⁴ We consider two sets of basis operators, $\mathbf{A} = (A^{(1)}, \dots, A^{(n)})^T$ and $\mathbf{B} = (B^{(1)}, \dots, B^{(n)})^T$, and the two-time retarded matrix Green's function $\mathbf{G}(\omega) = \langle\langle \mathbf{A}; \mathbf{B}^+ \rangle\rangle_\omega$. Separating from $i\dot{\mathbf{A}}$ the irreducible part \mathbf{I} , defined by $\langle\langle [\mathbf{I}, \mathbf{B}^+]_\eta \rangle\rangle = 0$ ($\eta = \pm$), i.e.,

$$i\dot{\mathbf{A}} = \Omega \mathbf{A} + \mathbf{I}, \quad (2)$$

we get the frequency matrix

$$\Omega = \mathbf{M}' \mathbf{M}^{-1} \quad (3)$$

with the spectral moments

$$\mathbf{M} = \langle\langle [\mathbf{A}, \mathbf{B}^+]_\eta \rangle\rangle, \quad \mathbf{M}' = \langle\langle [i\dot{\mathbf{A}}, \mathbf{B}^+]_\eta \rangle\rangle. \quad (4)$$

Defining the self-energy matrix by

$$\Sigma(\omega) = \langle\langle \mathbf{I}; \mathbf{B}^+ \rangle\rangle_\omega \mathbf{G}^{-1}(\omega), \quad (5)$$

the equation of motion yields

$$\mathbf{G}(\omega) = [\omega - \Omega - \Sigma(\omega)]^{-1} \mathbf{M}. \quad (6)$$

To express the self-energy in terms of a higher-order Green's function, the equation of motion for $\mathbf{G}'(\omega) = \langle\langle i\dot{\mathbf{A}}; \mathbf{B}^+ \rangle\rangle_\omega$ is used, where $\mathbf{G}'(\omega)$ is differentiated with respect to the second time. In this way, we obtain the exact representation

$$\Sigma(\omega) = \langle\langle i\dot{\mathbf{A}}; -i\dot{\mathbf{B}}^+ \rangle\rangle_\omega^{\text{irr}} \mathbf{M}^{-1} \quad (7)$$

with the irreducible Green's function

$$\langle\langle i\dot{\mathbf{A}}; -i\dot{\mathbf{B}}^+ \rangle\rangle_\omega^{\text{irr}} = \langle\langle i\dot{\mathbf{A}}; -i\dot{\mathbf{B}}^+ \rangle\rangle_\omega - \mathbf{G}'(\omega) \mathbf{G}^{-1}(\omega) \mathbf{G}'(\omega). \quad (8)$$

This projection method is equivalent to the Mori-Zwanzig projection technique^{14,15} and to the composite-operator approach,¹⁶ and it is closely related to the method of irreducible Green's functions¹⁷ and to the Roth method.¹⁸

Next, we employ the projection technique to calculate the dynamic spin susceptibility $\chi^{+-}(\mathbf{q}, \omega) = -\langle\langle S_{\mathbf{q}}^+; S_{-\mathbf{q}}^- \rangle\rangle_\omega$ [$\eta = -$, $\mathbf{S}_{\mathbf{q}} = (1/\sqrt{N}) \sum_i \mathbf{S}_i e^{-i\mathbf{q}\mathbf{R}_i}$] of the 2D Heisenberg model (1) over the whole temperature region. Hereafter, we put $J=1$ and the lattice spacing $a=1$. To take into account the AFM SRO and to preserve the spin-rotational symmetry, we choose the basis sets

$$\mathbf{A} = \mathbf{B} = (S_{\mathbf{q}}^+, iS_{\mathbf{q}}^+)^T. \quad (9)$$

Then, the Green's-function matrix $\mathbf{G}(\omega)$ has the elements

$$G_{\mathbf{q}}^{(11)} = \langle\langle S_{\mathbf{q}}^+; S_{-\mathbf{q}}^- \rangle\rangle_\omega, \quad G_{\mathbf{q}}^{(22)} = \langle\langle iS_{\mathbf{q}}^+; -iS_{-\mathbf{q}}^- \rangle\rangle_\omega, \quad (10)$$

$$G_{\mathbf{q}}^{(12)} = G_{\mathbf{q}}^{(21)} = \langle\langle iS_{\mathbf{q}}^+; S_{-\mathbf{q}}^- \rangle\rangle_\omega. \quad (11)$$

The moment matrices (4) are given by

$$\mathbf{M} = \begin{pmatrix} 0 & M_{\mathbf{q}}^{(1)} \\ M_{\mathbf{q}}^{(1)} & 0 \end{pmatrix}, \quad \mathbf{M}' = \begin{pmatrix} M_{\mathbf{q}}^{(1)} & 0 \\ 0 & M_{\mathbf{q}}^{(3)} \end{pmatrix}, \quad (12)$$

where

$$M_{\mathbf{q}}^{(1)} = \langle\langle [i\dot{S}_{\mathbf{q}}^+, S_{-\mathbf{q}}^-]_- \rangle\rangle, \quad (13)$$

$$M_{\mathbf{q}}^{(3)} = \langle\langle [-\ddot{S}_{\mathbf{q}}^+, -i\dot{S}_{-\mathbf{q}}^-]_- \rangle\rangle. \quad (14)$$

In Eq. (12), the spectral moments $M_{\mathbf{q}}^{(n)}$ with $n=0,2$ vanish due to the rotational symmetry ($\langle\langle S_{\mathbf{q}}^z \rangle\rangle = 0$). Neglecting in Eq. (6) the self-energy part, which defines a generalized mean-field approximation, by Eqs. (3) and (12)–(14) we obtain

$$\mathbf{G}(\omega) = \frac{1}{\omega^2 - \omega_{\mathbf{q}}^2} \begin{pmatrix} M_{\mathbf{q}}^{(1)} & M_{\mathbf{q}}^{(1)} \omega \\ M_{\mathbf{q}}^{(1)} \omega & M_{\mathbf{q}}^{(3)} \end{pmatrix}, \quad (15)$$

with the spin-excitation spectrum

$$\omega_{\mathbf{q}}^2 = M_{\mathbf{q}}^{(3)} / M_{\mathbf{q}}^{(1)}. \quad (16)$$

From Eq. (15) we get the dynamic spin susceptibility

$$\chi^{+-}(\mathbf{q}, \omega) = -\frac{M_{\mathbf{q}}^{(1)}}{2\omega_{\mathbf{q}}} \left(\frac{1}{\omega - \omega_{\mathbf{q}}} - \frac{1}{\omega + \omega_{\mathbf{q}}} \right), \quad (17)$$

the static spin susceptibility

$$\chi^{+-}(\mathbf{q}) = \frac{M_{\mathbf{q}}^{(1)}}{\omega_{\mathbf{q}}^2}, \quad (18)$$

and the equal-time two-spin correlation function

$$C_{\mathbf{q}} = \langle S_{\mathbf{q}}^+ S_{-\mathbf{q}}^- \rangle = \frac{M_{\mathbf{q}}^{(1)}}{2\omega_{\mathbf{q}}} [1 + 2n(\omega_{\mathbf{q}})], \quad (19)$$

where $n(\omega_{\mathbf{q}}) = (e^{\omega_{\mathbf{q}}/T} - 1)^{-1}$ is the Bose function. From Eq. (19) the spin-correlation functions

$$C_{\mathbf{R}} = \langle S_0^+ S_{\mathbf{R}}^- \rangle = \frac{1}{N} \sum_{\mathbf{q}} C_{\mathbf{q}} \cos \mathbf{q}\mathbf{R} \quad (20)$$

of arbitrary range $\mathbf{R} = n\mathbf{e}_x + m\mathbf{e}_y$ can be determined. Hereafter, we denote $C_{\mathbf{R}} \equiv C_{n,m}$. The nearest-neighbor correlation function is directly related to the internal energy per site by $u = 3C_{1,0}$.

Now we calculate the spectral moments in terms of two-spin correlation functions. For $M_{\mathbf{q}}^{(1)}$ we get

$$M_{\mathbf{q}}^{(1)} = -8C_{1,0}(1 - \gamma_{\mathbf{q}}), \quad (21)$$

where $\gamma_{\mathbf{q}} = \frac{1}{2}(\cos q_x + \cos q_y)$.

To calculate $M_{\mathbf{q}}^{(3)} = M_{\mathbf{q}}^{(1)} \omega_{\mathbf{q}}^2$ we take the site representation of Eq. (14), where \ddot{S}_i^+ contains products of three spin operators along nearest-neighbor sequences. We decouple \ddot{S}_i^+ in the spirit of the Green's-function approach by Shimahara and Takada.¹¹ Considering, for example, the product $S_i^+ S_j^+ S_l^-$, we introduce the vertex parameters α_i ($i=1,2,3$) as follows:

$$S_i^+ S_j^+ S_l^- = \alpha_\nu \langle S_j^+ S_l^- \rangle S_i^+ + \alpha_3 \langle S_i^+ S_l^- \rangle S_j^+. \quad (22)$$

Here, α_ν ($\nu=1,2$) is attached to nearest-neighbor correlation functions, where α_1 (α_2) is taken if $\langle i,j,l \rangle$ forms a nearest-neighbor sequence along a line (triangle), and α_3 is associated with the further-distant correlation functions. As com-

pared to Ref. 11 (α_2 of Ref. 11 is equal to α_3), our decoupling (22) is extended by the introduction of the additional parameter $\alpha_2 \neq \alpha_1$.

Finally, we obtain

$$\omega_{\mathbf{q}}^2 = \lambda_0(1 - \gamma_{\mathbf{q}}) + \lambda_1(\gamma_{\mathbf{q}} - \gamma'_{\mathbf{q}}) + \lambda_2(\gamma_{\mathbf{q}} - \gamma_{2\mathbf{q}}) \quad (23)$$

with

$$\lambda_0 = 2 + 4\alpha_3(C_{2,0} + 2C_{1,1}), \quad (24)$$

$$\lambda_1 = -8\alpha_2 C_{1,0}, \quad \lambda_2 = -4\alpha_1 C_{1,0}, \quad (25)$$

and $\gamma'_{\mathbf{q}} = \cos q_x \cos q_y$.

We have checked that our scheme preserves the spin-rotation invariance. That is, the calculation of the longitudinal susceptibility using the basis sets $\mathbf{A} = \mathbf{B} = (S_{\mathbf{q}}^z, iS_{\mathbf{q}}^z)^T$ yields $\chi^{zz}(\mathbf{q}, \omega) \equiv \chi(\mathbf{q}, \omega) = \frac{1}{2} \chi^{+-}(\mathbf{q}, \omega)$.

By Eqs. (18), (21), and (23) we get the uniform static spin susceptibility $\chi(T) = \lim_{\mathbf{q} \rightarrow 0} \chi(\mathbf{q})$,

$$\chi(T) = -2C_{1,0} [1 + 2\alpha_3(C_{2,0} + 2C_{1,1}) - 2C_{1,0}(3\alpha_1 + 2\alpha_2)]^{-1}. \quad (26)$$

From the expansion of $\chi(\mathbf{q})$ around the AFM wave vector $\mathbf{Q} = (\pi, \pi)$ we obtain the AFM correlation length $\xi(T)$,

$$\xi^2 = \frac{\lambda_0 + \lambda_2 - \Delta}{4\Delta}, \quad (27)$$

where

$$\Delta = \lambda_0 - \lambda_1 - \lambda_2 = \frac{1}{2} \omega_{\mathbf{Q}}^2. \quad (28)$$

The theory has six temperature-dependent parameters ($C_{1,0}, C_{1,1}, C_{2,0}; \alpha_1, \alpha_2, \alpha_3$) and four self-consistency equations (20) which include the sum rule $C_{0,0} = 1/2$. The two remaining conditions are detailed in Sec. III.

Our Green's-function projection approach is closely related to previous isotropic spin-wave theories.^{11,12,19} This can be seen by the simplified version of the decoupling (22) in which the dependence on the relative site position of the vertex parameters α_ν is neglected; i.e., $\alpha_2 = \alpha_1$. From Eq. (23) we get

$$\omega_{\mathbf{q}}^2 = (\lambda_0 + \lambda_2)(1 - \gamma_{\mathbf{q}}) \left(1 + \frac{4\lambda_2}{\lambda_0 + \lambda_2} \gamma_{\mathbf{q}} \right), \quad (29)$$

since $2\gamma'_{\mathbf{q}} + \gamma_{2\mathbf{q}} = 4\gamma_{\mathbf{q}}^2 - 1$. Thus, the \mathbf{q} dependence of all quantities is governed by $\gamma_{\mathbf{q}}$ only. By the choice $\alpha_2 = \alpha_1$, the results of the Green's-function decoupling scheme by Shimahara and Takada¹¹ may be obtained. The final expressions of the isotropic linear spin-wave theory by Sokol *et al.*¹² agree with our analytical results, if the parameters C_1 and C_2 of Ref. 12 are formally identified as $C_1 = \frac{1}{8} [1 + 2\alpha_3(C_{2,0} + 2C_{1,1}) - 2\alpha_1 C_{1,0}]$ and $C_2 = \alpha_1 C_{1,0}$, respectively. Note that in the composite-operator approach of Ref. 19 the moment $M_{\mathbf{q}}^{(3)}$ was not calculated, but parametrized by an ansatz compatible with the shape of Eq. (29).

III. GROUND-STATE PROPERTIES

The critical behavior of the 2D Heisenberg model (1) is reflected in our theory [cf. Eq. (18)] by the closure of the spectrum gap at \mathbf{Q} as $T \rightarrow 0$, so that $\lim_{T \rightarrow 0} \chi^{-1}(\mathbf{Q}) = 0$. From $\omega_{\mathbf{Q}} = 0$, i.e., by Eq. (28) $\Delta = 0$, we obtain the condition

$$1 + 2\alpha_3(C_{2,0} + 2C_{1,1}) = -2C_{1,0}(\alpha_1 + 2\alpha_2), \quad (30)$$

and the spin-wave excitation spectrum

$$\omega_{\mathbf{q}}^2 = -4C_{1,0} [\alpha_1(1 - \gamma_{2\mathbf{q}}) + 2\alpha_2(1 - \gamma'_{\mathbf{q}})]. \quad (31)$$

For $q \equiv |\mathbf{q}| \ll 1$ we have

$$\omega_{\mathbf{q}} = 2\sqrt{-C_{1,0}(\alpha_1 + \alpha_2)}q, \quad (32)$$

with the spin-wave velocity (c_s) renormalization factor $Z_c = c_s/\sqrt{2} = \sqrt{-2C_{1,0}(\alpha_1 + \alpha_2)}$. By Eqs. (26) and (30) we get

$$\chi = \frac{1}{4(\alpha_1 + \alpha_2)}. \quad (33)$$

To calculate the correlation functions (20) with Eq. (19) at $T=0$, we separate the condensation part C , arising from $\omega_{\mathbf{Q}} = 0$, as follows:

$$C_{\mathbf{R}} = \frac{1}{N} \sum_{\mathbf{q}} \frac{M_{\mathbf{q}}^{(1)}}{2\omega_{\mathbf{q}}} \cos \mathbf{qR} + C \cos \mathbf{QR}. \quad (34)$$

From the sum rule and Eqs. (21) and (31) we have

$$C = \frac{1}{2} - 2\sqrt{-C_{1,0}} \frac{1}{N} \sum_{\mathbf{q}} I_{\mathbf{q}} \quad (35)$$

with

$$I_{\mathbf{q}} = (1 - \gamma_{\mathbf{q}}) [\alpha_1(1 - \gamma_{2\mathbf{q}}) + 2\alpha_2(1 - \gamma'_{\mathbf{q}})]^{-1/2}. \quad (36)$$

By Eqs. (34) and (35) we get

$$C_{\mathbf{R}} = \frac{1}{2} \cos \mathbf{QR} + 2\sqrt{-C_{1,0}} K_{\mathbf{R}}, \quad (37)$$

where

$$K_{\mathbf{R}} = \frac{1}{N} \sum_{\mathbf{q}} I_{\mathbf{q}} (\cos \mathbf{qR} - \cos \mathbf{QR}). \quad (38)$$

From Eq. (37) the nearest-neighbor correlation function is obtained as

$$C_{1,0} = - \left(\sqrt{K_{1,0}^2 + \frac{1}{2}} - K_{1,0} \right)^2. \quad (39)$$

The staggered magnetization m is calculated from Eq. (34) according to

$$m^2 = \lim_{|\mathbf{R}| \rightarrow \infty} \langle \mathbf{S}_0 \mathbf{S}_{\mathbf{R}} \rangle \cos \mathbf{QR} = \frac{3}{2} C \quad (40)$$

with C given by Eq. (35). We see that, at $T=0$, all quantities may be expressed as functions of the vertex parameters α_1 and α_2 .

In the case $\alpha_2 = \alpha_1$ (cf. Sec. II), Eq. (31) yields the spectrum

TABLE I. Ground-state properties (see text) compared with Monte Carlo data and other approaches.

	MC	Case 1	Case 2	Ref. 11	Ref. 12
u	-0.6693 (Ref. 20)	-0.7032	-0.6693	-0.7016	-0.6701
m	0.3074 (Ref. 20)	0.3134	0.2641	0.3000	0.2519
χ	0.0446 (Ref. 21)	0.0495	0.0569	0.0534	0.0604

$$\omega_{\mathbf{q}}^2 = -16\alpha_1 C_{1,0}(1 - \gamma_{\mathbf{q}}^2) \quad (41)$$

which has the same shape as in traditional spin-wave theory.⁵

To determine α_1 and α_2 at zero temperature, we take the MC data for the ground-state energy per site, $u = 3C_{1,0}$,²⁰ the staggered magnetization m ,²⁰ and the rotationally averaged uniform static susceptibility χ at $T=0$ [obtained from the susceptibility renormalization factor $Z_\chi = 12\chi = 0.535$ (Ref. 21)] which are listed in Table I. Inserting those quantities into Eqs. (39), (40), and (33) we get the relations between $\alpha_1(0)$ and $\alpha_2(0)$ depicted in Fig. 1. The choice $\alpha_2 = \alpha_1$ discussed in Sec. II (where either m^{11} or u^{12} are used as input quantities) and the unphysical region $C_{2,0} > C_{1,1}$ below the dashed line are also indicated. As can be seen, there is no parameter choice which likewise fits u , m , and χ . However, the shaded area marks the region of appropriate $\alpha(0)$ values. To formulate conditions also at finite temperatures, where all vertex parameters are temperature dependent, we express the two unknown parameters (by analogy with Ref. 11) in terms of the ratios $r_{\alpha_i} = [\alpha_i(T) - 1] / [\alpha_1(T) - 1]$ ($i=2,3$), since all vertex parameters are suggested to approach unity at high temperatures. We treat two cases for the choice of r_{α_2} and r_{α_3} . In case 1, we choose the center of the shaded area in Fig. 1, i.e., $\alpha_1(0) = 3.055$ and $\alpha_2(0) = 1.998$, yielding by Eqs. (30) and (37), $\alpha_3(0) = 2.634$. Moreover, we assume r_{α_2} and r_{α_3} as temperature independent. In case 2, we keep r_{α_2} from case 1 and take the MC data on $u(T)$ (Refs. 20 and 22) to determine $r_{\alpha_3}(T)$ [at $T=0$, we get $\alpha_1(0) = 2.610$, $\alpha_2(0) = 1.782$, $\alpha_3(0) = 2.237$; cf. Fig. 1].

To sum up, in the evaluation of our theory over the whole temperature region we adopt the following conditions.

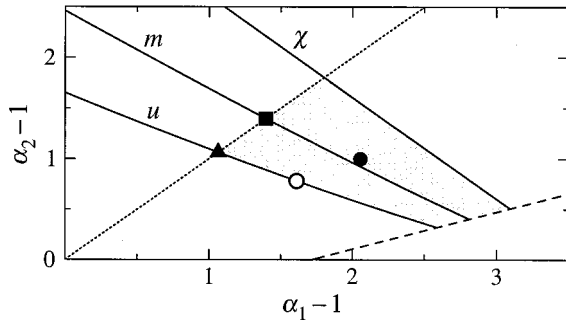


FIG. 1. Relations between the vertex parameters α_1 and α_2 at $T=0$ for given Monte Carlo data on u , m , and χ (cf. Table I). The choices in case 1 (●), case 2 (○), Ref. 11 (■), and Ref. 12 (▲) are indicated. The dotted and dashed lines refer to $\alpha_2 = \alpha_1$ and $C_{2,0} = C_{1,1}$, respectively.

(i) Case 1:

$$r_{\alpha_2} = \frac{\alpha_2(T) - 1}{\alpha_1(T) - 1} = 0.4856,$$

$$r_{\alpha_3} = \frac{\alpha_3(T) - 1}{\alpha_1(T) - 1} = 0.7951. \quad (42)$$

(ii) Case 2:

$$r_{\alpha_2} = 0.4856,$$

$$r_{\alpha_3}(T) \text{ from } u_{\text{MC}}(T). \quad (43)$$

In Table I our ground-state results for u , m , and χ are given and compared with the MC data and the results of Refs. 11 and 12. Let us point out that in contrast to the approach by Sokol *et al.*,¹² our values for the staggered magnetization and the zero-temperature susceptibility in case 1 are much closer to the MC data.

Considering spin correlations of arbitrary range, we have evaluated the correlation function (37) and compared the results for $\tilde{C}_{\mathbf{R}} = \langle \mathbf{S}_0 \mathbf{S}_{\mathbf{R}} \rangle = \frac{3}{2} C_{\mathbf{R}}$ with the projector MC (PMC) data by Liang.²³ As shown in Table II, our theory reproduces the PMC results within an average deviation of about 2% (13%) in case 2 (case 1).

Finally, let us consider the spin-wave spectrum (31) with the shape $\omega_{\mathbf{q}}/Z_c$ shown in Fig. 2. Contrary to the conventional shape $\omega_{\mathbf{q}} \sim (1 - \gamma_{\mathbf{q}}^2)^{1/2}$ [cf. Eq. (41)], our theory with $\alpha_2 \neq \alpha_1$ yields a slight minimum in $\omega_{\mathbf{q}}$ at $\mathbf{q} = (\pi, 0)$. On the other hand, Chen *et al.*²⁴ have suggested from their PMC data that the exact spectrum has the conventional form (41). This was also found by Krüger and Schuck²⁵ using a non-spin-rotation-invariant projection method, where $Z_c = 1.188$ agrees with the MC value of Ref. 20. In case 1 (case 2) we get $Z_c = 1.539$ (1.400), as compared to $Z_c = 1.480$ and $Z_c = 1.360$ obtained by Shimahara and Takada¹¹ and Sokol *et al.*,¹² respectively. Those results indicate that our spin-rotation-invariant theory of SRO is less appropriate to de-

TABLE II. Spin-correlation functions $\tilde{C}_{\mathbf{R}} = \langle \mathbf{S}_0 \mathbf{S}_{\mathbf{R}} \rangle$ at $T=0$ compared with projector Monte Carlo data (Ref. 23).

	PMC	Case 1	Case 2
$\tilde{C}_{1,0}$	-0.3348	-0.3516	-0.3347
$\tilde{C}_{1,1}$	0.2028	0.2247	0.2028
$\tilde{C}_{2,0}$	0.1772	0.2069	0.1830
$\tilde{C}_{2,1}$	-0.1671	-0.1906	-0.1665
$\tilde{C}_{2,2}$	0.1475	0.1683	0.1431
$\tilde{C}_{3,0}$	-0.1491	-0.1706	-0.1454
$\tilde{C}_{3,1}$	0.1430	0.1626	0.1371

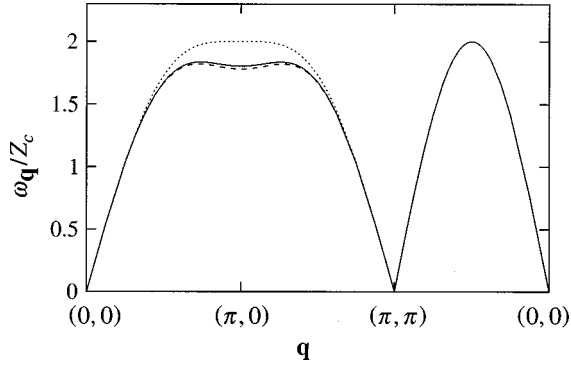


FIG. 2. Spin-wave spectrum at $T=0$ in case 1 (dashed), case 2 (solid), and in conventional spin-wave theory (dotted). In each case the results are scaled as $\omega_{\mathbf{q}}/Z_c$.

scribe the excitation spectrum, but, as shown in Sec. IV, it is more suitable for the description of thermodynamic properties and correlation functions of arbitrary range over the whole temperature region (note that the approach of Ref. 25 yields $|u|=0.264$ at $T=0$ and does not allow the calculation of further-distant correlation functions).

IV. FINITE-TEMPERATURE RESULTS

At nonzero temperatures ($m=0$) we have solved the self-consistency equations (20) supplemented by conditions (42) or (43) to obtain the static spin susceptibility $\chi(\mathbf{q})$ for arbitrary \mathbf{q} , the AFM correlation length $\xi(T)$, the spin structure factor $C_{\mathbf{q}}$, and the two-spin correlation functions $C_{\mathbf{R}}$ of arbitrary range. The vertex parameters are found to decrease with increasing temperature approaching unity at high temperatures (cf. Sec. III).

Our results for the uniform static susceptibility (26) are shown in Fig. 3. In view of the susceptibility behavior over the whole temperature region in comparison with the MC data,²² cases 1 and 2 yield an improved description of the low-temperature susceptibility as compared with Refs. 11 and 12, respectively. The increase of χ with temperature, the

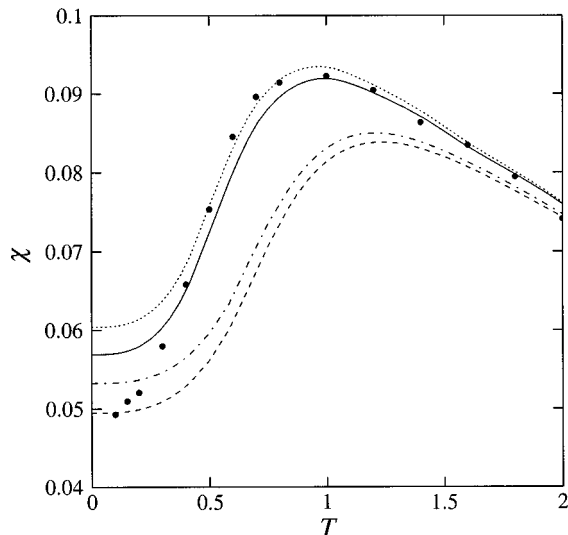


FIG. 3. Uniform spin susceptibility in the cases 1 (dashed) and 2 (solid) compared with MC data (●, Ref. 22) and the approaches of Ref. 11 (chain-dashed) and Ref. 12 (dotted).

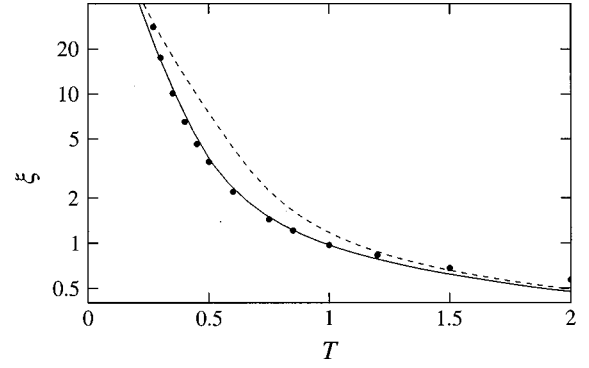


FIG. 4. Antiferromagnetic correlation length in the cases 1 (dashed) and 2 (solid) compared with the MC data (●) of Ref. 26.

maximum near the exchange energy, and the crossover to the high-temperature Curie-Weiss behavior are due to the decrease of AFM SRO with increasing temperature (see below).

In Fig. 4 the AFM correlation length $\xi(T)$ given by Eq. (27) is depicted, where in case 2 a very good agreement with the MC results²⁶ at intermediate temperatures is found. To obtain the low-temperature expansion of $\xi(T)$ up to the leading order, we expand the Bose contribution to $C_{\mathbf{q}}$ in Eq. (19) around the AFM wave vector \mathbf{Q} . As $T \rightarrow 0$, this contribution yields the condensation part of $C_{\mathbf{R}}$ [Eq. (34)] and determines the leading order of Δ and of the correlation length. We obtain

$$\xi = 2 \sqrt{[\alpha_1(0) + \alpha_2(0)] |C_{1,0}(0)|} \frac{1}{T} \times \exp \left[\frac{\pi}{3} [\alpha_1(0) + \alpha_2(0)] \frac{m^2}{T} \right]. \quad (44)$$

Compared with the full temperature dependence of ξ calculated by Eq. (27), the expansion (44) holds up to $T=0.2$ within a deviation of 9%. Note that the preexponential factor T^{-1} is an artifact of the mean-field approach. On the basis of the nonlinear σ model, Chakravarty *et al.*⁶ have shown that the preexponential becomes a temperature-independent prefactor, if a two-loop renormalization-group correction is taken into account.

The AFM structure factor $\tilde{C}_{\mathbf{Q}} = \langle \mathbf{S}_{\mathbf{Q}} \mathbf{S}_{-\mathbf{Q}} \rangle = \frac{3}{2} C_{\mathbf{Q}}$ is plotted in Fig. 5 as a function of $T^2 \xi^2$, since the renormalization-

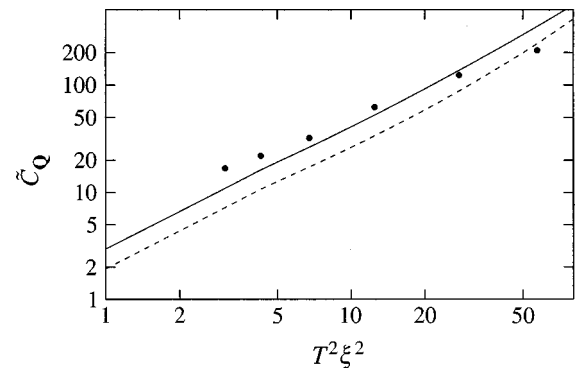


FIG. 5. Antiferromagnetic structure factor $\tilde{C}_{\mathbf{Q}} = \frac{3}{2} C_{\mathbf{Q}}$ vs $T^2 \xi^2$ in cases 1 (dashed) and 2 (solid) compared with MC data (●, Ref. 26).

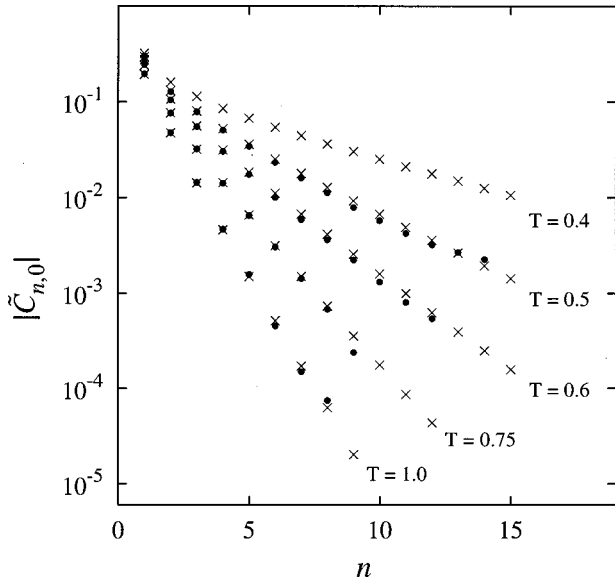


FIG. 6. Spin-correlation functions $|\tilde{C}_{n,0}|$ in case 2 (\times) at different temperatures in comparison with the MC data (\bullet) of Ref. 26.

group analysis of the classical nonlinear σ model predicts the scaling form $\tilde{C}_{\mathbf{Q}} \propto T^2 \xi^2$.⁶ Our results in both cases 1 and 2 reproduce reasonably well the scaling behavior, where in case 2 the agreement with the MC data²⁶ is satisfying. Concerning the relation between $\tilde{C}_{\mathbf{Q}}$ and the staggered susceptibility $\chi(\mathbf{Q})$, at high ($\beta\omega_{\mathbf{q}} \ll 1$) and low temperatures ($\beta\omega_{\mathbf{q}} \ll 1$ due to the exponentially small spectrum gap $\omega_{\mathbf{Q}} = \sqrt{2\Delta}$), the expansion of Eq. (19) compared with Eq. (18) yields $\tilde{C}_{\mathbf{Q}} = 3T\chi(\mathbf{Q})$.

To see in more detail the characteristics of AFM SRO as a function of spatial range and temperature, in Fig. 6 the magnitude of $\tilde{C}_{\mathbf{R}} = \langle \mathbf{S}_0 \mathbf{S}_{\mathbf{R}} \rangle$ with $\mathbf{R} = (n, 0)$ is depicted in case 2. As can be seen, the decrease of SRO with increasing temperature is described in excellent agreement with the MC data of Ref. 26.

Finally, let us compare our theory with experiments on La_2CuO_4 . Taking the recent neutron-scattering data for the correlation length by Birgeneau *et al.*³ in the range $340 < T \leq 820$ K, we have determined the free parameter J by a least-squares fit shown in Fig. 7. We obtain ($a = 3.79 \text{ \AA}$)

$$J = \begin{cases} 108 \text{ meV,} & \text{case 1,} \\ 133 \text{ meV,} & \text{case 2.} \end{cases} \quad (45)$$

Thereby, we have calculated $\xi(T)$ by Eq. (27) instead of using the low-temperature expansion (44) which is only valid, according to Eq. (45), below about 300 K. Our values for the exchange energy agree very well with those obtained from the comparison of numerical approaches with experiments [$J = 133 \text{ meV}$ (Ref. 20) from $\hbar c_s = 1.68Ja = 850 \text{ meV \AA}$ and $J = 125 \text{ meV}$ (Ref. 26) from the fit of $\xi_{\text{MC}}(T)$]. On the contrary, in previous analytical approaches, the deduced values of J are found to be too low [$J = 78 \text{ meV}$ (Ref. 8) and $J = 86 \text{ meV}$ (Ref. 11)].

As seen in Fig. 7, at $T > 500$ K we obtain a very good quantitative agreement with experiments. Such an agreement was also found by Birgeneau *et al.*³ in the comparison of their data with the theory by Hasenfratz and Niedermeyer,⁷ if

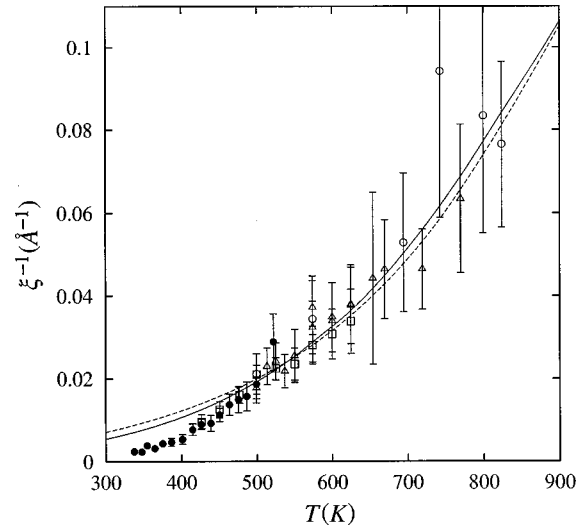


FIG. 7. Inverse antiferromagnetic correlation length in La_2CuO_4 obtained by the neutron-scattering experiments of Ref. 3 (\circ , \triangle , \square , \bullet) and from the fit of the theory in case 1 (dashed) and case 2 (solid).

the relations between c_s , ρ_s , and J with $J = 135 \text{ meV}$ are used. Moreover, the excellent agreement of the neutron-scattering data with the theory of Ref. 7 extends down to 340 K. The deviation of our results from the Birgeneau *et al.*³ data below 500 K (cf. Fig. 7) is due to the appearance of the preexponential factor T^{-1} in Eq. (44).

As to the maximum in the uniform static spin susceptibility of La_2CuO_4 , we determine the maximum temperature T_{max} from Fig. 3 using the values of J given by Eq. (45). Thus, without any further fit, we get

$$T_{\text{max}} = \begin{cases} 1545 \text{ K,} & \text{case 1,} \\ 1535 \text{ K,} & \text{case 2.} \end{cases} \quad (46)$$

Those values agree rather well with the estimate given by Johnston,⁴ $T_{\text{max}} = 1460 \text{ K}$, by means of a scaling analysis of the susceptibility data below 800 K.

Considering both the correlation length and the magnetic susceptibility of La_2CuO_4 , our theory reasonably agrees with experiments. Whereas the nonlinear- σ -model approach^{6,7} yields a better agreement with the $\xi(T)$ data below 500 K, as compared with our results (cf. Fig. 7), the maximum in the magnetic susceptibility cannot be described within the theory by Chakravarty *et al.*,⁶ since it is only valid at $T \ll 2\pi\rho_s$ [$2\pi\rho_s = 1.169J$ (Ref. 20) $\approx 1800 \text{ K}$].

V. SUMMARY

The basic ingredients of our spin-rotation-invariant theory of short-range order (SRO) in the 2D Heisenberg antiferromagnet are the following.

(i) The Green's-function projection technique is used, where a two-operator basis (spin and its first time derivative) is chosen and a generalized mean-field approximation is employed to calculate the dynamic spin susceptibility over the whole temperature region.

(ii) The SRO is described in terms of two-spin correlation functions of arbitrary range. Thereby, the third spectral moment is decoupled by use of vertex parameters.

(iii) The system of self-consistency equations is completed by the choice of appropriate vertex-parameter conditions.

Our approach provides a systematic treatment of spin correlations. In particular, a more detailed analysis than in Ref. 11 is given. In contrast to the mean-field approaches of Refs. 11 and 12, our theory allows a straightforward extension taking into account self-energy effects.

The theory is numerically evaluated at arbitrary temperatures and wave vectors. The main results are summarized as follows.

(i) The uniform static spin susceptibility (revealing a maximum near the exchange energy and a crossover to the Curie-Weiss law) exhibits an improved interpolation between the low-temperature and high-temperature behavior, as compared with previous isotropic spin-wave approaches.

(ii) The theory describes the spin correlations (correlation length, pair-correlation functions) in very good agreement with Monte Carlo data.

(iii) The comparison with neutron-scattering experiments on La_2CuO_4 shows good quantitative agreement, where the fit of the exchange energy yields $J = 133$ meV. The temperature of the maximum in the magnetic susceptibility of La_2CuO_4 agrees rather well with the experimental estimate.

The good quantitative agreement of our theory with experiments emphasizes the role of a strong SRO in the cuprates. We conclude that the extension of the Green's-function projection theory to the t - J model may be promising to describe the doping dependence of SRO and its effects on the unconventional magnetic properties of high- T_c compounds.

ACKNOWLEDGMENTS

We wish to thank H. Fehske and A. Kühnel for valuable discussions.

* Author to whom correspondence should be addressed.

Electronic address: steffen.winterfeldt@itp.uni-leipzig.de

¹For a review, see A. P. Kampf, Phys. Rep. **249**, 219 (1994).

²G. Shirane, R. J. Birgeneau, Y. Endoh, and M. A. Kastner, Physica B **197**, 158 (1994).

³R. J. Birgeneau *et al.*, J. Phys. Chem. Solids **56**, 1913 (1995).

⁴D. C. Johnston, Phys. Rev. Lett. **62**, 957 (1989); T. Nakano *et al.*, Phys. Rev. B **49**, 16 000 (1994).

⁵For reviews, see E. Manousakis, Rev. Mod. Phys. **63**, 1 (1991); T. Barnes Int. J. Mod. Phys. C **2**, 659 (1991).

⁶S. Chakravarty, B. I. Halperin, and D. R. Nelson, Phys. Rev. B **39**, 2344 (1989).

⁷P. Hasenfratz and F. Niedermayer, Phys. Lett. B **268**, 231 (1991).

⁸M. Takahashi, Phys. Rev. B **40**, 2494 (1989).

⁹J. E. Hirsch and S. Tang, Phys. Rev. B **40**, 4769 (1989); S. Tang, M. E. Lazzouni, and J. E. Hirsch, *ibid.* **40**, 5000 (1989).

¹⁰D. P. Arovas and A. Auerbach, Phys. Rev. B **38**, 316 (1988); A. Auerbach and D. P. Arovas, Phys. Rev. Lett. **61**, 617 (1988).

¹¹H. Shimahara and S. Takada, J. Phys. Soc. Jpn. **60**, 2394 (1991).

¹²A. Sokol, R. R. P. Singh, and N. Elstner, Phys. Rev. Lett. **76**, 4416 (1996).

¹³H. Shimahara and S. Takada, J. Phys. Soc. Jpn. **61**, 989 (1992).

¹⁴Yu. A. Tserkovnikov, Theor. Math. Phys. **50**, 171 (1982); A.

Belkasri and J. L. Richard, Phys. Rev. B **50**, 12 896 (1994).

¹⁵P. Fulde, *Electron Correlations in Molecules and Solids*, 3rd ed., Springer Series in Solid State Sciences, Vol. 100 (Springer, Berlin, 1995).

¹⁶H. Matsumoto, M. Sasaki, S. Ishihara, and H. Tachiki, Phys. Rev. B **46**, 3009 (1992); F. Mancini, S. Marra, A. M. Allega, and H. Matsumoto, in *Superconductivity and Strongly Correlated Electronic Systems*, edited by C. Noce, A. Romano, and G. Scarpetta (World Scientific, Singapore, 1994), p. 271.

¹⁷N. M. Plakida, Phys. Lett. **43A**, 481 (1973).

¹⁸L. M. Roth, Phys. Rev. **184**, 451 (1969); J. Beenen and D. M. Edwards, Phys. Rev. B **52**, 13 636 (1995).

¹⁹A. M. Allega, S. Odashima, H. Matsumoto, and F. Mancini, Physica C **235-240**, 2229 (1994).

²⁰U.-J. Wiese and H.-P. Ying, Z. Phys. B **93**, 147 (1994).

²¹K. J. Runge, Phys. Rev. B **45**, 12 292 (1992).

²²Y. Okabe and M. Kikuchi, J. Phys. Soc. Jpn. **57**, 4351 (1988).

²³S. Liang, Phys. Rev. B **42**, 6555 (1990).

²⁴G. Chen, H.-Q. Ding, and W. A. Goddard, Phys. Rev. B **46**, 2933 (1992).

²⁵P. Krüger and P. Schuck, Europhys. Lett. **27**, 395 (1994).

²⁶M. S. Makivić and H.-Q. Ding, Phys. Rev. B **43**, 3562 (1991).